Implication of sulfonylurea derivatives as prospective inhibitors of human carbonic anhydrase II

Danish Idrees, Murtuza Hadianawala, Amarjyoti Das Mahapatra, Bhaskar Datta, Sonam Roy, Shahzaib Ahamad, Parvez Khan, Md. Imtiyaz Hassan

PII: S0141-8130(18)30632-9
DOI: doi:10.1016/j.ijbiomac.2018.04.131
Reference: BIOMAC 9539

To appear in:

Received date: 6 February 2018
Revised date: 23 April 2018
Accepted date: 24 April 2018

Please cite this article as: Danish Idrees, Murtuza Hadianawala, Amarjyoti Das Mahapatra, Bhaskar Datta, Sonam Roy, Shahzaib Ahamad, Parvez Khan, Md. Imtiyaz Hassan , Implication of sulfonylurea derivatives as prospective inhibitors of human carbonic anhydrase II. The address for the corresponding author was captured as affiliation for all authors. Please check if appropriate. Biomac(2017), doi:10.1016/j.ijbiomac.2018.04.131

Running head: Sulfonylurea derivatives as CAII Inhibitors

Implication of sulfonylurea derivatives as prospective inhibitors of human carbonic anhydrase II

Danish Idrees[1], Murtuza Hadianawala[2], Amarjyoti Das Mahapatra[2], Bhaskar Datta[2,*], Sonam Roy[1], Shahzaib Ahamad[3], Parvez Khan[1] and Md. Imtiyaz Hassan[1*]

[1]*Centre for Interdisciplinary Research in Basic Sciences, Jamia Millia Islamia, Jamia Nagar, New Delhi 110025, India.*
[2]*Department of Chemistry, Indian Institute of Technology, Palaj, Gandhinagar, Gujarat - 382355, India.*
[3]*Department of Biotechnology, College of Engineering & Technology, IFTM University, Lodhipur-Rajput, Delhi Road, Moradabad, India.*

*** All correspondence should be addressed to,**

Md. Imtiyaz Hassan, Ph.D.
E-mail: mihassan@jmi.ac.in

Bhaskar Datta, Ph.D.
E-mail: bdatta@iitgn.ac.in

ABSTRACT

Selective carbonic anhydrase (CA) inhibitors have gained a lot of importance owing to the implication of specific isoforms of CA in certain diseases like glaucoma, leukemia, cystic fibrosis, and epilepsy. A novel class of sulfonylurea derivatives was synthesized from corresponding sulfonyl chlorides and amines. Compounds with different pendant moieties in the sulfonylurea derivatives show significant interactions with human carbonic anhydrase II (CAII). *In vitro* evaluation of the sulfonylurea derivatives revealed three compounds possessing admirable inhibitory activity against CAII. Compounds containing methyl (**G2**), isopropyl (**G4**) and o-tosyl (**G5**) groups displayed IC_{50} (109-137 μm) for CAII. Fluorescence binding and cytotoxicity studies revealed that these compounds are showing good binding affinity (18-34 μM) to CAII and non- toxic to cells. Further, Molecular docking studies of G2, G4 and G5 with CAII showed these compounds fit nicely in the active site of CAII. Molecular dynamics simulation studies of these compounds complexed with CAII also showed essential interactions which were maintained up to 50 ns of simulation. These results indicate the promising nature of the sulfonylurea scaffold towards CAII inhibition and opens scope of hit to-lead optimization for discovery of effective drugs against CAII-associated disorders.

***Keywords**:* Carbonic anhydrase, Sulfonyl urea derivatives, Enzyme inhibition, Structure based drug design

1. Introduction

Carbonic anhydrases (CA, EC.4.2.1.1) catalyze the reversible hydration of carbon dioxide (CO_2) and enable regulation of pH of living system [1-3]. These are metalloenzymes predominantly possess zinc(II) in the active site cavity which is essential for their enzymatic activities [4, 5]. There are 16 isoforms of CA which are distributed to almost all organelle of human body and are essential for varieties of cellular processes [2, 6]. Apart from their main cellular function, inhibition of these isozymes is used to address a wide range of disease conditions including glaucoma to cancer [7-11].

Sulphanilamide is one of the earliest reported and widely applicable CA inhibitors [12]. Elucidation of the sulphonamide group as a Zn(II) binding entity spurred the development of CA inhibitors (CAIs) with a modular architecture. CAIs have been designed and developed with a zinc binding group (ZBG), an aromatic scaffold and a capping group or tail segment [12, 13]. The aromatic scaffold and tail ensure better positioning of the ZBG [14]. CAIs possessing such modular architectures have been implicated in the direct coordination to Zn(II) in the active site or to Zn(II)-bound solvent molecules as part of their mechanism of action [8, 15]. While such a design paradigm has resulted in large numbers of CAIs, poor isozyme selectivity has prevented their wider clinical application [12, 16]. Several new classes of compounds such as coumarins and phenols have been identified for their ability to bind at the entrance of the CA active site [17, 18] to manifest in the inhibition of CA [18, 19].

Attempts have been made to combine the strengths of the two approaches to CA inhibition, namely, interaction with Zn(II) and active site entrance blockage [20]. However, such strategies met with a little success [21]. For example, sulfonamide-containing CAIs have been designed

with sugar-containing tail segments for targeting specific isozymes [22, 23]. Unfortunately, such anomeric sulphonamides do not exhibit differences in K_is between the cytosolic CAII and the membrane-associated isozyme CAIX [24]. In this context, several bioisosters of sulphonamides such as sulfamates and sulfamides have also been explored as CAIs [25, 26]. While many of these have been identified as tight-binding inhibitors, isozyme-specificity as an innate trait has remained elusive.

Interestingly, the sulfonylurea group is a bioisostere of sulphonamide which has received scant attention for use in CAIs. We have recently reported sulfonylurea-derivatives as inhibitors of CAII [27]. CAII is a ubiquitous isozyme of CA and creates challenges for selective targeting of tumor-specific isozymes (CAIX and CAXII). We already reported the structural and biophysical properties of different CAs [28-31]. Here, we report sulfonylurea-derivatives for their ability for effective CAII inhibition in nm range. Three molecules (**G2, G4** and **G5**) have been identified with micromolar IC_{50}s. Binding mode analysis by molecular docking reveals an interesting association of these sulfonylurea-derivatives in the active site of the enzyme. Notably, hydrogen bonding and hydrophobic interactions are observed with several key active site residues such as His64, Asn67, Thr199 and Thr200. The present study highlights sulfonylurea as a novel scaffold for effective CAII inhibition and expands the scope for discovery of effective drugs against epilepsy and glaucoma.

2. Materials and methods

2.1. Synthesis of sulfonylurea

Benzenesulfonyl chloride (0.5 g, 2.8 mmol) was treated with pyridine (0.4 mL, 5.0 mmol) and allowed to stir for 5 min. The resultant solution was transferred to a mixture of sodium cyanate (0.25 g, 3.9 mmol) in acetonitrile (5 mL) and allowed to stir for about 4 hour at room temperature. To the resultant mixture aniline (0.364 mL, 4 mmol) was added and the stirred for about 1 hr at room temperature. The resulting reaction mixture was poured on crushed ice and acidified with dil HCl (pH 5 - 6). Aqueous layer was extracted with ethyl acetate three times and combined extract was washed with brine and dried over anhydrous Na_2SO_4. Solvent was evaporated under vacuum and resulting residue was further purified by column chromatography to afford a white solid compound G7 (125 mg, 20%).

^{1}H NMR ($CDCl_3$, 500 MHz): δ 8.47 (brs, 1H, NH), 7.95 (d, 2H, *J* = 7.5 Hz), 7.65 (t, 1H, *J* = 7.5 Hz), 7.54 (t, 2H, *J* = 7.5 Hz), 7.4 (d, 2H, *J* = 8 Hz), 7.32 (t, 2H, *J* = 7.5 Hz), 7.14 (t, 1H, *J* = 7.5 Hz); ^{13}C NMR ($CDCl_3$, 125 MHz): 148.57, 139.51, 136.55, 134.06, 129.58, 129.18, 126.89, 124.94, 120.40; MS (ESI): 277.093 [M+H]+, 299.07 $[M+Na]^+$

2.2. Synthesis of thiosulfonylurea-derivatives

To (970.6 mg, 4.6 mmol) p-Chlorobenzenesulfonyl chloride, 10 ml aqueous ammonium hydroxide was added and refluxed for 1 h. Reaction mixture was then quenched with water and acidified with dil HCl (pH 5 - 6). The resulting product was filtered, dissolved in DCM and dried over anhydrous Na_2SO_4. Solvent was evaporated under vacuum and resulting residue was used for the next step without further purification. To a solution of the sulfonamide (1.00 mmol) in DMF, KO^{t}Bu (1.20 mmol) was added and stirred for 15 min. To this solution phenylisocyanate (0.6 mL, 5.5 mmol) was added and heated at 80 °C for 1 h. Reaction mixture was quenched with

water and acidified with dil HCl (pH 5-6). Product was isolated by filtration and was further purified using flash chromatography to yield title compound G8 (1.1 g, 74%).

^{1}H NMR ($CDCl_3$, 500 MHz): δ 9.65 (brs, 1H, NH), 8.19 (brs, 1H, NH), 7.88 (d, 2H, *J* = 8.5 Hz), 7.57 (d, 2H, *J* = 8.5 Hz), 7.46 (d, 2H, *J* = 8.0 Hz), 7.39 (t, 2H, *J* = 8.0 Hz), 7.29 (t, 1H, *J* = 8.0 Hz); ^{13}C NMR(CDC_{l3}, 125 MHz): 176.49, 141.31, 137.15, 136.88, 130.07, 129.18, 128.55, 127.41, 124.29; MS (ESI): 327.00 $[M+H]^+$

2.3. Carbonic anhydrase inhibition assay

The inhibitory action of synthesized compounds was measured by esterase assay against CAII using earlier described methods (28, 30). The esterase activity of CAII was measured by following the change in absorbance at 400 nm of p-nitrophenyl acetate(4-NPA) to 4-nitrophenolate ion over a period of 3 min at 25°C using a spectrophotometer Jasco UV/visible spectrophotometer (Jasco V-660, Model B 028661152). Reaction mixture contained 50 mM Tris buffer (pH 8.0), 100 mM NaCl, 1 mM EDTA, and 3 mM substrate p-nitrophenol acetate. 1µM of protein concentration was used and different concentrations of synthesized compounds were used in a total volume of 500µl. A reference measurement was obtained by preparing the same reagents in cuvette without enzyme solution. The synthesized compounds were tested in triplicate at each concentration used. Control enzyme activity in the absence of a drug was taken as 100%. Acetazolamide (AZM) was used as a reference compound. The IC_{50} values for each synthesized compounds were calculated by using GraphPad Prism (Version 5.0) graphing software.

2.4. Fluorescence binding study

The binding study of compounds (G2, G4 and G5) with CAII protein was performed by monitoring the changes in fluorescence intensity of protein. All fluorescence measurement was

performed in the Jasco spectrofluorimeter (Model FP-6200) using 5 mm quartz cuvette (excitation at 292 nm, emission at 300–400 nm). Protein concentration of 1 µM CAII and compounds were used in a concentration 1–10 µM. Compounds were dissolved in DMSO and then diluted to 1 mg/ml in the 50 mM Tris pH 8.0 and 150 mM NaCl. The protein solution was titrated with increasing concentration of compounds. The decrease in fluorescence intensity is due to the increasing concentration of compounds has been used to calculate the binding affinity by Stern–Volmer equations with slight modification.

$$\log (Fo - F)/F = \log Ka + n\log[Q] \quad (1)$$

Where Fo is the fluorescence intensity of protein and F is the fluorescence intensity of ligand, Ka is the binding constant and n is the number of binding sites, Q represents quenching constant. For the ligand–protein complex, the values for Ka and n can be derived from the intercept and slope.

2.5. Cell culture and cytotoxicity assay

HEK293 cell lines were routinely maintained and cultured in a 5% CO_2 humidified incubator at 37°C, in DMEM supplemented with 10% heat inactivated fetal bovine serum (Gibco), 1% penicillin, streptomycin solution (Gibco). Cells were routinely maintained and trypsinized not more than 30 passages. To see the cytotoxicity of synthesized compounds on cell viability and proliferation, standard MTT assay was used as described earlier [32, 33]. Briefly, cells were seeded (8000-9000/well) in a 96-well plate and allowed to grow overnight. On the next day, cells were treated with increasing concentrations (5–200 µM) of studied compounds in a final volume of 200 µl for 24 and 48 h at 37º C in a humidified CO_2 incubator. At the end of the treeatment, 20 µl of MTT solution and 100 µl of DMEM (from 5mg/ml stock solution in PBS) was added to each well and incubated for 4-5 h at 37ºC in a humidified CO_2 incubator. Finally the supernatant

was aspirated and the colored formazan crystal produced from MTT was dissolved in 150µl of DMSO. The absorbance was measured at 570 nm with the help of multiplate ELSIA reader (BioRad). The percentage of cell viability was calculated and plotted as a function of concentration of compound.

2.6. Docking studies

Molecular docking approaches have been used to know the binding mode of ligand and receptor in drug discovery. We have used Autodock (version 4.2), an automated tool to perform docking which was installed on Windows 7 OS (on HP Proliant DL180 G6 workstation) [34-36]. We have used crystal structure of human carbonic anhydrase II (CAII) (PDB-ID: 1CA2). 2D chemical structures of the ligand was drawn and converted into 3D structure by using Chemdraw version 12 and utilized MMP2 and MM2 force-field to energy minimize the compounds. After energy minimization compound G2, G4 and G5 required to convert into docking input file format (i.e. .pdb to .pdbqt), ligands and protein files converted into .pdbqt. The ligands was docked into the cavity site of CAII protein, when we employ the auto-grid box dimensions were set to be 126 x 126 x 126 Å of XYZ axes and default grid point spacing of 0.375 Å was established by using the Auto-Grid module. To predict the bounded conformation based on the empirical force filed Lamerckian Genetic Algorithm (LGA) runs was performed [37]. After completion of docking run all the compounds .dlg file were analyzed to know the binding pattern with protein. We applied blind docking approach for the docking of 1CA2, further we also used CASTp server to predict the binding site of protein. The autodock4 predicted the binding exactly at the binding site as predicted by castp (CASTp server widely used server know the protein binding pockets) [38]. PyMOL software was used to visualize the protein ligand binding site

[39]. Finally, docking results provide good binding free energy that forms stable complexes between CAII and compound G2, G4 and G5 by forming hydrogen bonding.

2.7. MD Simulations

The general methodology of MD simulations was carried out on CAII and complex with compound G2, G4 and G5 using GROMSCS-Version 4.6.5 (on HP Proliant DL580 G7 workstation). The topology of CAII was produced on the basis of GROMOS96 53A6 force-field [40]. Due to the lack of suitable force field parameters for drug molecules in the GROMACS software package, PRODRG server [41] is a program for generation of molecular topologies and coordinate files. After creating the topology, coordinate file of compound G2, G4 and G5 were immersed into SPC/E (model) water box of cubic shape. In this mode, counter ions was added for entire system neutralized. In order to neutralized system and energetically minimized via two methods steepest descent and conjugate gradient algorithms (CGA) converged criterion within of 0.005 kcal mol^{-1}. To increase the reliability of MD simulations apply restrain both the drug and protein structure before the equilibration phase. Once equilibration phase was done separately in constant temperature (300 K), constant volume ensemble (NVT) as well as constant temperature (300K), constant pressure (NPT) conditions, appropriate time scale for each 100 ps. By keeping the native binding coordinate condition of ligand and protein restrained. Nose Hoover thermostat and Parrinello-Rahman barostat (1 bar) were maintained temperature and pressure ensemble, respectively. Finally, the MD simulation production with 300 K temperature and each of the independent trajectories used 50 ns (LINCS Algorithm). Each complex behavior, at time step of 2fs was used in water environment. The knowledge of analyzed the MD trajectories Root Mean Square Deviation (RMSD), radius of gyration (*R*g), root means square fluctuations (RMSF) and

secondary structure content were developed by Do_dssp program. In this study, we performed 50 ns (50,000 ps) MD simulations of WT CAII, compound G2, G4 and G5. The totaling of 200 ns of trajectories analysis was calculated for the protein backbone with respect to the initial conformation.

3. Results and Discussion

3.1.Synthesis and characterization of sulfonylurea and thiosulfonylurea-derivatives

Sulfonylurea derivatives are widely used in anti-diabetic medicines. These have been traditionally prepared by the treatment of sulphonamide with appropriate isocyanate in presence of base [42]. We have recently reported a general method for synthesis of sulfonylurea derivatives from sulfonyl chlorides and amines [43]. The same method was used for synthesis of several compounds in this work (**Scheme 1 and Table 1**).

In each case the sulfonyl chloride was first treated with pyridine followed by addition of sodium cyanate and reaction with the suitable amine. However, the single-pot reaction was ineffective for the synthesis of thiosulfonylurea derivatives. These were synthesized by the conventional approach of first converting the sulfonyl chloride into sulphonamide followed by reaction with isothiocyanate. The yield of the single-pot method ranged from modest to comparable in contrast to the conventional approach (**Scheme 2 and Table 2**). Nevertheless, the hazardous nature of the conventional approach as well as the wider scope afforded by the direct use of sulfonyl chlorides and amines maintains the attractive nature of the single-pot method. The final compounds were obtained as solids and were purified and characterized using standard techniques. Stock solutions of the sulfonylurea and thiosulfonylurea-derivatives were prepared in DMSO and used for biological assays. The synthesized compounds were characterized by ^{1}H NMR, ^{13}C NMR and

mass spectroscopy. The purity of the target compounds was evaluated by elemental analysis (see **supplementary data**).

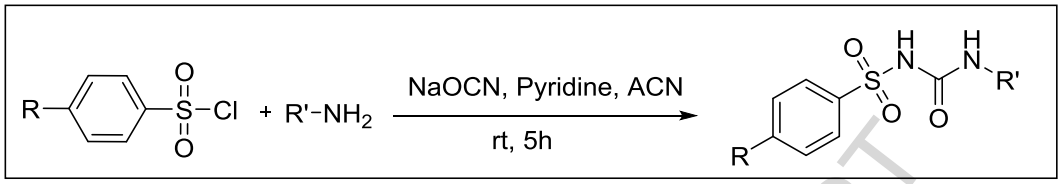

Molecule #	R	R’
G1	-CH_3	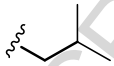
G2	-CH_3	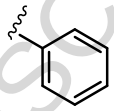
G3	-CH_3	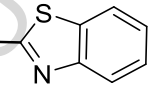
G6	-Cl	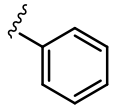
G7	-H	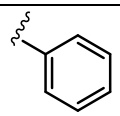

Scheme 1. Synthesis of sulfonylureas G1-3, 6 and 7

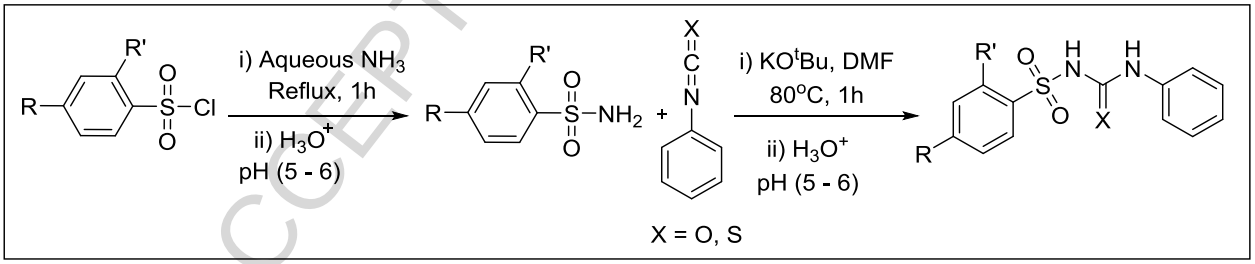

Compound	R	R’
G4		-H
G5	-H	-CH_3
G8	-Cl	-H
G9	-H	-H

Scheme 2. Synthesis of sulfonylureas G4, G5, G8 and G9

3.2.CAII inhibition assay

The inhibition studies of synthesized compounds against CAII were carried out using the esterase activity assay of CA, with p-nitrophenyl acetate (4-NPA) as a substrate which is colorless. The inhibitory activity of compounds against CAII is shown in **Table 3**. Compounds G2, G4 and G5 show good inhibition of CAII. All these compounds have phenyl rings at the two ends of the sulfonylurea moiety with various alkyl substitutions. The importance of the phenyl groups is most evident from a comparison of performance with compounds G1 and G3. A less bulky isobutyl (**G1**) or an aromatic but bulkier benzothiazole (G3) are unable to provide suitable bonding contacts with the enzyme site. Within the molecules with phenyl rings at the terminal ends of sulfonylurea the combination of methyl and phenyl (G2), 4-Isopropyl and phenyl (G4) and o-methyl and phenyl group (G5) led to the most profound inhibition of CAII with compound G2 having IC_{50} = 137.41 μm, compound G4 having IC_{50} = 109.34 μm and compound G5 have IC_{50} = 125.62 μm. The good inhibition by compounds G2, G4 and G5 is indicative of the important interactions effected by the phenyl rings with the alkyl substitutions providing suitable interaction with the enzyme active site. Interestingly, use of the thiosulfonylurea compounds G8 and G9 do not lead to any significant differences in CAII inhibition as compared to their sulfonylurea counterparts G6 and G7. These results point to the structural scaffold provided by phenyl substituted sulfonylurea as a promising new class of selective CAII inhibitors.

3.3.Fluorescence binding studies

The fluorescence emission spectra of CAII solutions in the absence and presence of different concentrations of compounds in Tris at 25°C are recorded. The maximum emission peak of CAII was observed at 343 nm (excitation wavelength was 292 nm). Upon incubation of different

concentrations (1–10 µM) of compounds with CAII the maximum fluorescence peak intensity was reduced significantly indicating that CAII formed complexes with compounds. The change in the intrinsic fluorescence intensity of CAII was observed when compounds bind to them. The values fluorescence intensity at 343 nm was plotted as a function of [ligand] to calculate the binding affinity of compounds against CAII (**Figure 1**). The fluorescence quenching results were observed for CAII with compounds but the binding affinities of compounds (G4 and G5) are comparatively high than compound (G2). The binding affinity of compounds for CAII is 34.20 µM, 18.57 µM, and 19.21 µM (**Table 4**).

3.4.Cytotoxicity studies

Three selected compounds (G2, G4 and G5) were evaluated on HEK-293 cell lines by MTT assay. These compounds were screened in the concentration range of 0-200 µM, and treatments were given for 24 and 48 h. The results shown that compound G2, G4 and G5 does not elicit any towards HEK-293 cell lines **(Figure 2)**. Cytotoxicity of these compounds for HEK-293 cells were also studied at their respective IC_{50} (from enzyme inhibition assay) value for 72 h, we observed that more than 90% embryonic kidney cells were viable even after 72 h of incubation (data not shown). Results from cytotoxicity studies clearly indicate that the studied compounds are non-toxic to HEK-293 cells.

3.5.Molecular docking studies

Molecular docking studies are widely used for predicting the binding study and inhibition constant (K_i) of compounds. In this study, CAII was docked with Compounds G2, G4 and G5 to elucidate their interaction patterns. Result suggested that the compounds G2, G4 and G5 are

nicely bounded into the active site of CAII with lowest binding energy reported in **Table 4**. The G2 in the active site of CAII is stabilized with six H-bond interaction with Asn62, His64, and Asn67 (**Figure 3A**). The G4 in the active site of CAII is stabilized with three H-bond interactions with Asn62, His64, Gln92 and Thr200 (**Figure 3B**). Furthermore, G**5** is stabilized by six H-bond interactions with His64, Asn67 Gln92 and Thr200 (**Figure 3C**).

Finally docking study concluded that the compounds G2, G4 and G5 have showed good binding energy value of □7.32, □7.56 and □6.69 (Δ*G* in kcal/mol), respectively (see **Table 4)**. The inhibitory constant, binding energy for CAII and these compounds may be considered as candidate in development of selective CAII inhibitor.

3.6.MD Simulation

MD simulation analysis of CAII and ligand-bound with compounds G2, G4 and G5 are indicated in black, red, green and blue, respectively. The average RMSD values computing know the protein stability in-terms of backbone RMSD *vs* time (ps) of 50 ns each. The observed RMSD of only CAII increases till ~5 ns fluctuate ~0.1 nm and then achieved the equilibrium, 15 to 30 ns quite disrupt the RMSD and remains stable throughout the simulation. Results suggest that the CAII remain stable during the MD simulation, the average RMSD calculated 0.16 nm. WT and all other compound comparatively achieved equilibrium approximately ~5 ns of the MD simulation. Maximum fluctuation occurs with G5, after equilibration RMSD sharply increased at ~ 12 ns and stable till 30 ns. However, another fluctuation increase at 30 ns then stabilized protein throughout the simulation and the average RMSD is 0.30. From **Figure 4** the average RMSD value of WT and all the complexes are reported in **Table 5**. These results suggested that the G4 have least average RMSD value 0.21

as compare to all other compounds. Similar results found in docking study that provide lowest binding energy -7.56 stabilize the protein complex with G4.

The R_g is measurement of compactness of CAII and complexed with compounds G2, G4 and G5 represented in **Figure 5**. The *R*g value of WT comparatively to all the compound are less than WT, that suggesting compounds provides significant compactness and rigidity to the protein and thus increasing the complex stability. The Average *R*g values are mention in **Table 5**.

Structural mobility analysis plays a key role in MD simulation which is analyzed through g_rmsf module of gromacs. The flexibility of protein structure from **Figure 6** illustrate the RMSF of residues was plotted in the presence of compounds G2, G4 and G5. We observed that the G2 at residues 8-10 (loops region) increases fluctuation ~5 nm and residues 18-20, 125-130 (α-helices region) fluctuation bars reaches ~ 3.0 nm and 200-204 (loops region) fluctuation bars ~3.0 nm. Similarly, compound G5 shown at residues 22-24 (α-helices region) fluctuation bars 3.5, residues 100-105 (loops region), 171-173 (??-sheets region) fluctuation bars ~2.5 nm and 235-240 (loops region) ~3.0 nm. Finally, compound G4 displays the least fluctuations as compare to other compounds, the residues 53-58 (loops region) only ~2.0 nm. The RMSF plot clearly indicates that the G4 stabilize CAII as compared to other compounds, similar result found in RMSD.

Protein functionality is affected by tertiary as well as secondary structure. Investigation of secondary structure provide an idea about the conformation changes of whole protein structures in each time scale from the entire MD trajectory (**Figure 7A-D)**. Secondary structure changes in the presence of different compounds are described in **Table 6**. Major

protein component of secondary structure like ??-sheets content and helices increases in the presence of G4. Moreover, in the case of G2 and G5 helices decreases. In the case of compound G4 a considerable increase was observed as compared to other compounds, and suggesting maximum stability to protein.

Conclusions

A new series of compounds incorporating the sulfonylurea and sulfonylthiourea moieties have been prepared and investigated for their interaction with human CAII. Several molecules in this class were identified as having CAII inhibitory activity. In particular, the biological evaluation of these compounds reveals good inhibitory activity of compounds G2, G4 and G5. These compounds were also found to exhibit good binding affinity for CAII. The present molecules represent a promising structural motif that can be further explored for enhancing isoform selective inhibition of CA. In particular, the currently reported molecules may constitute interesting candidates for the development of novel antiepileptic strategies.

Acknowledgement: DI thanks to the University Grants Commission for the award of fellowship. This work is supported by Council of Scientific and Industrial Research, India (Grant No. 37(1665)/15/EMR-II). B.D. is grateful to Center for Biomedical Engineering, IIT Gandhinagar for financial support of this work.

References

[1] W.S. Sly, P.Y. Hu, Human carbonic anhydrases and carbonic anhydrase deficiencies, Annu. Rev. Biochem. 64 (1995) 375-401.

[2] C.T. Supuran, Carbonic anhydrases - an overview, Current Pharmaceutical Design 14 (2008) 603- 614.

[3] M. Imtaiyaz Hassan, B. Shajee, A. Waheed, F. Ahmad, W.S. Sly, Structure, function and applications of carbonic anhydrase isozymes, Bioorg Med Chem 21(6) (2013) 1570-82.

[4] K.S. Smith, C. Jakubzick, T.S. Whittam, J.G. Ferry, Proc. Natl. Acad. Sci. USA 96 (1999) 15184.

[5] Y. Xu, L. Feng, P.D. Jeffrey, Y. Shi, F.M. Morel, Nature 452 (2008) 56.

[6] D. Hewett-Emmett, The Carbonic Anhydrases - New Horizons, Birkhauser Verlag, Basel, 2000, pp. 29 - 78.

[7] C.T. Supuran, A. Scozzafava, Carbonic anhydrase inhibitors, Current Medicinal Chemistry 1 (2001) 61 - 97.

[8] C.T. Supuran, Carbonic anhydrases: novel therapeutic applications for inhibitors and activators, Nature Reviews Drug Discovery 7 (2008) 168 - 181.

[9] C.T. Supuran, Carbonic anhydrase inhibitors, Bioorganic & Medicinal Chemistry Letters 20 (2010) 3467 - 3474.

[10] S. Kumari, D. Idrees, C.B. Mishra, A. Prakash, Wahiduzzaman, F. Ahmad, M.I. Hassan, M. Tiwari, Design and synthesis of a novel class of carbonic anhydrase-IX inhibitor 1-(3-(phenyl/4-fluorophenyl)-7-imino-3H-[1,2,3]triazolo[4,5d]pyrimidin 6(7H)yl)urea, J Mol Graph Model 64 (2016) 101-109.

[11] S. Kumari, C.B. Mishra, D. Idrees, A. Prakash, R. Yadav, M.I. Hassan, M. Tiwari, Design, synthesis, in silico and biological evaluation of novel 2-(4-(4-substituted piperazin-1-yl)benzylidene)hydrazine carboxamides, Mol Divers 21(1) (2017) 163-174.

[12] C.T. Supuran, A. Scozzafava, A. Casini, Carbonic anhydrase inhibitors, Medicinal Research Reviews 23 (2003) 146 - 189.

[13] S. Pastorekova, S. Parkkila, J. Pastorek, C.T. Supuran, Carbonic Anhydrases: Current State of the Art, Therapeutic Applications and Future Prospects, Journal of Enzyme Inhibition and Medicinal Chemistry 19 (2004) 199 - 229.

[14] C.T. Supuran, A. Scozzafava, Curr. Med. Chem. - Imm. Endoc. Metab. Agents 1 (2001) 61 - 97.

[15] S.K. Nair, P.A. Ludwig, D.W. Christianson, Two-site binding of phenol in the active site of human carbonic anhydrase II: structural implications for substrate association, J. Am. Chem. Soc. 116 (1994) 3659-3660.

[16] C.T. Supuran, A. Scozzafava, Exp. Opin. Ther. Patents 10 (2000) 575 - 600.

[17] A. Innocenti, D. Vullo, A. Scozzafava, C.T. Supuran, Carbonic anhydrase inhibitors: interactions of phenols with the 12 catalytically active mammalian isoforms (CA I - XIV), Bioorganic & Medicinal Chemistry Letters 18 (2008) 1583 - 1587.

[18] A. Maresca, C. Temperini, L. Pochet, B. Masereel, A. Scozzafava, C.T. Supuran, Deciphering the mechanism of carbonic anhydrase inhibition with coumarins and thiocoumarins, J. Med. Chem. 53 (2010) 335 - 344.

[19] C. Temperini, A. Innocenti, A. Scozzafava, S. Parkkila, C.T. Supuran, The Coumarin-binding site in carbonic anhydrase accommodates structurally diverse inhibitors: The antiepileptic lacosamide as an example and lead molecule for novel classes of carbonic anhydrase inhibitors, J. Med. Chem. 53 (2010) 850 - 854.

[20] A.L. Banerjee, D. Eiler, B.C. Roy, X. Jia, M.K. Haldar, S. Mallik, O.K. Srivastava, Spacer-based selectivity in the binding of "two-prong" ligands to recombinant human carbonic anhydrase I, Biochemistry 44 (2005) 3211 - 3224.

[21] D. Vomasta, A. Innocenti, B. Konig, C.T. Supuran, Carbonic anhydrase inhibitors: two-prong versus mono-prong inhibitors of isoforms I, II, IX, and XII exemplified by photochromic cis-1,2-alpha-dithienylethene derivatives, Bioorganic & Medicinal Chemistry Letters 19 (2009) 1283 - 1286.

[22] J.Y. Winum, S.A. Poulsen, C.T. Supuran, Therapeutic applications of glycosidic carbonic anhydrase inhibitors, Medicinal Research Reviews 29 (2009) 419 - 435.

[23] J.Y. Winum, P.A. Colinas, C.T. Supuran, Glycosidic carbonic anhydrase IX inhibitors: A sweet approach against cancer, Bioorganic & MEdicinal Chemistry 21 (2013) 1419 - 1426.

[24] M. Lopez, B. Paul, A. Hofmann, J. Morizzi, Q.K. Wu, S.A. Charman, A. Innocenti, D. Vullo, C.T. Supuran, S.A. Poulsen, S-glycosyl primary sulfonamides--a new structural class for selective inhibition of cancer-associated carbonic anhydrases, J. Med. Chem. 52 (2009) 6421 - 6432.

[25] O.M. Rodriguez, A. Maresca, C.A. Tempera, R.D. Bravo, P.A. Colinas, C.T. Supuran, N-β-glycosyl sulfamides are selective inhibitors of the cancer associated carbonic anhydrase isoforms IX and XII, Bioorganic & Medicinal Chemistry Letters 21 (2011) 4447 - 4450.

[26] M. Lopez, J. Trajkovic, L.F. Bornaghi, A. Innocenti, D. Vullo, C.T. Supuran, S.A. Poulsen, Design, synthesis, and biological evaluation of novel carbohydrate-based sulfamates as carbonic anhydrase inhibitors, J. Med. Chem. 54 (2011) 1481 - 1489.

[27] M. Hadianawala, B. Datta, Design and development of sulfonylurea derivatives as zinc metalloenzyme modulators, RSC Advances 6 (2016) 8923 - 8929.

[28] D. Idrees, A. Prakash, M.A. Haque, A. Islam, F. Ahmad, M.I. Hassan, Spectroscopic and MD simulation studies on unfolding processes of mitochondrial carbonic anhydrase VA induced by urea, J Biomol Struct Dyn 34(9) (2016) 1987-97.

[29] D. Idrees, A. Prakash, M.A. Haque, A. Islam, M.I. Hassan, F. Ahmad, GdnHCl-induced unfolding intermediate in the mitochondrial carbonic anhydrase VA, Int J Biol Macromol 91 (2016) 1151-60.

[30] D. Idrees, M. Shahbaaz, K. Bisetty, A. Islam, F. Ahmad, M.I. Hassan, Effect of pH on structure, function, and stability of mitochondrial carbonic anhydrase VA, J Biomol Struct Dyn 35(2) (2016) 449-461.

[31] A. Prakash, D. Idrees, M.A. Haque, A. Islam, F. Ahmad, M.I. Hassan, GdmCl-induced unfolding studies of human carbonic anhydrase IX: a combined spectroscopic and MD simulation approach, J Biomol Struct Dyn (2016) 1-12.

[32] P. Khan, S. Rahman, A. Queen, S. Manzoor, F. Naz, G.M. Hasan, S. Luqman, J. Kim, A. Islam, F. Ahmad, M.I. Hassan, Elucidation of Dietary Polyphenolics as Potential Inhibitor of Microtubule Affinity Regulating Kinase 4: In silico and In vitro Studies, Sci Rep 7(1) (2017) 9470.

[33] A. Queen, P. Khan, D. Idrees, A. Azam, M.I. Hassan, Biological evaluation of p-toluene sulphonylhydrazone as carbonic anhydrase IX inhibitors: An approach to fight hypoxia-induced tumors, Int J Biol Macromol (2017).

[34] W.E.H. Forli, S. Halliday, R. Belew, A.J. Olson, AutoDock Version 4.2.

[35] E. Jameel, H. Naz, P. Khan, M. Tarique, J. Kumar, S. Mumtazuddin, S. Ahamad, A. Islam, F. Ahmad, N. Hoda, Design, synthesis, and biological evaluation of pyrimidine derivatives as potential inhibitors of human calcium/calmodulin-dependent protein kinase IV, Chemical biology & drug design 89(5) (2017) 741-754.

[36] H. Naz, M. Tarique, P. Khan, S. Luqman, S. Ahamad, A. Islam, F. Ahmad, M.I. Hassan, Evidence of vanillin binding to CAMKIV explains the anti-cancer mechanism in human hepatic carcinoma and neuroblastoma cells, Molecular and Cellular Biochemistry (2017) 1-11.

[37] G.M. Morris, D.S. Goodsell, R.S. Halliday, R. Huey, W.E. Hart, R.K. Belew, A.J. Olson, Automated docking using a Lamarckian genetic algorithm and an empirical binding free energy function, Journal of computational chemistry 19(14) (1998) 1639-1662.

[38] J. Dundas, Z. Ouyang, J. Tseng, A. Binkowski, Y. Turpaz, J. Liang, CASTp: computed atlas of surface topography of proteins with structural and topographical mapping of functionally annotated residues, Nucleic acids research 34(suppl_2) (2006) W116-W118.

[39] W.L. DeLano, The PyMOL molecular graphics system, http://pymol. org (2002).

[40] D. Van Der Spoel, E. Lindahl, B. Hess, G. Groenhof, A.E. Mark, H.J. Berendsen, GROMACS: fast, flexible, and free, Journal of computational chemistry 26(16) (2005) 1701-1718.

[41] A.W. SchuÈttelkopf, D.M. Van Aalten, PRODRG: a tool for high-throughput crystallography of protein–ligand complexes, Acta Crystallographica Section D: Biological Crystallography 60(8) (2004) 1355-1363.

[42] J. Cervello, T. Sastre, Synthesis 1990 (1990) 221 - 222.

[43] M. Hadianawala, A. Shaik, N. Hasija, A.K. Vasu, B. Datta, Sodium Cyanate Mediated Synthesis of Sulfonylurea and Sulfonyltriuret from Sulfonyl Chloride and Amine, ChemistrySelect 1 (2016) 2212 - 2216.

Table 1: List of synthesized sulfonylureas G1 – G3, G6 and G7

Compound	R	R’	Yield (%)
G1	—≋	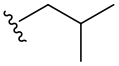	52
G2	—≋	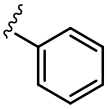	59
G3	—≋	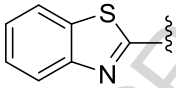	41
G6	Cl	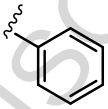	25
G7	H	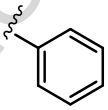	20

Table 2: List of synthesized sulfonylureas of G4, G5, G8 and G9

Compound	R/R’	X	Yield (%)
G4	Isopropyl / H	O	81
G5	H / CH3	O	52
G8	Cl / H	S	74
G9	H / H	S	77

Table 3: *In vitro* carbonic anhydrase inhibitory activity

Compound	Structure of compound	Name of Structures	IC50 (µM)
G1	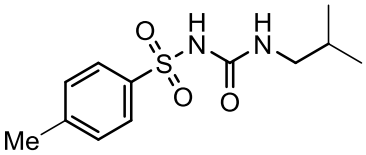	**N-(isobutylcarbamoyl)-4-methylbenzenesulfonamide**	339.60
G2	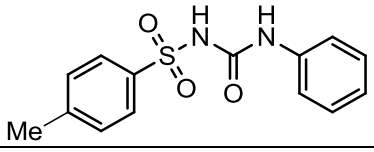	**4-methyl-N-(phenylcarbamoyl)benzenesulfonamide**	270.41
G3	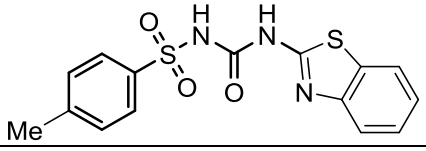	**N-(benzo[d]thiazol-2-ylcarbamoyl)-4-methylbenzenesulfonamide**	880.74
G4	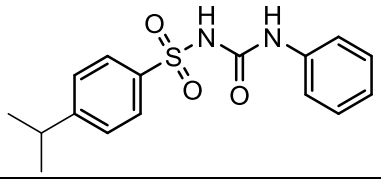	**4-isopropyl-N-(phenylcarbamoyl)benzenesulfonamide**	170.34
G5	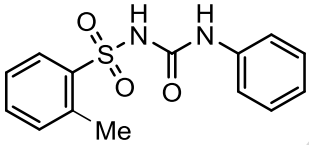	**2-methyl-N-(phenylcarbamoyl)benzenesulfonamide**	225.62
G6	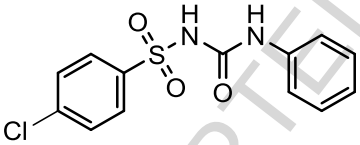	**4-chloro-N-(phenylcarbamoyl)benzenesulfonamide**	439.18
G7	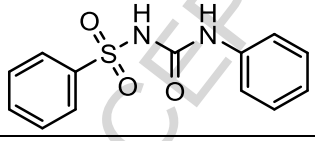	**N-(phenylcarbamoyl)benzenesulfonamide**	391.83
G8	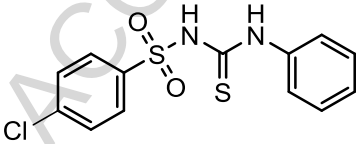	**4-chloro-N-(phenylcarbamothioyl)benzenesulfonamide**	421.59
G9	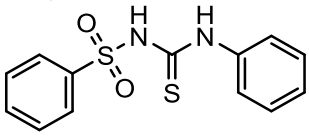	**N-(phenylcarbamothioyl)benzenesulfonamide**	383.63

Table 4: Binding parameters of each complex

Docked complex CAII-Compounds	Binding free energy (Δ*G* in kcal/mol)	Electrostatic Energy (kcal/mol)	Estimated Inhibition Constant Ki (μM)	vdW + Hbond + desolv Energy (kcal/mol)	*Binding affinity
G2	-7.32	-0.19	3.09	-8.52	34.20 μM
G4	-7.56	-0.11	4.05	-8.44	18.57 μM
G5	-6.69	-0.07	12.55	-7.51	19.21 μM

**calculated from fluorescence binding study*

Table 5: The average RMSD and R_g of WT-CAII and complex with CAII-compound G2, G4 and G5 during the 50 ns MD simulation.

Compounds No.	Average RMSD	Average *R*g
WT-CAII	0.16±0.01	1.74±0.01
G2	0.29±0.01	1.67±0.01
G4	0.21±0.01	1.67±0.01
G5	0.30±0.01	1.68±0.01

Table 6: The secondary structure plot representing structural content WT-CAII and complex compound G2, G4 and G5 at 300 K of 50 ns MD simulation.

Secondary structure compounds No.	structure	β-sheet	Coil	β-bridge	Bend	Turn	α-helix
WT-CAII	136.3	75.8	78.3	7.2	39.9	20.5	32.7
G2	135.7	79.3	70.9	7.3	43.8	25.6	23.3
G4	136.6	76.0	72.7	7.2	45.4	26.4	29.8
G5	140.3	82.6	71.6	6.9	40.8	23.4	27.3

Figure Legends

Figure 1: Fluorescence emission spectra of (A) CAII with G4, (B) plot of log (Fo− F)/F vs log [Q] for quenching of CAII by G4.

Figure 2: Cell viability assay. (A) Effect of CAII inhibitors on the viability of human normal cell (HEK-293) lines: Cells were treated with increasing concentrations of each compound (0-200 μM) for 48 h.

Figure 3: Surface representation of CAII docked with all three compounds G2, G4 and G5 in the same active site pocket and hydrophobic core of active site is colored with element. **(A)** Cartoon view of compound G2 docked with CAII, active site residue interactions with compound G2. Residues are shown with stick and compound G2 is shown with ball and stick model, hydrogen bonds are shown as broken lines (black). (**B)** Cartoon view of compound G4 docked with CAII. Interactions of active site residue with compound G4. Residues are shown with stick and compound G4 is shown with ball and stick model. **(C)** Cartoon view of compound G5 docked with CAII. Interactions of site residue with compound G5. Hydrogen bonds are shown as broken lines (black).

Figure 4: RMSD plot of CAII trajectories analysis produced by Gromacs; CAII (black), compound G2 (red), compound G4 (green) and compound G5 (blue).

Figure 5: R_g plot of MD trajectories produced by Gromacs; CAII (black), compound G2 (red), compound G4 (green) and compound G5 (blue).

Figure 6: RMSF plot, trajectories produced by Gromacs; CAII (black), compound G2 (red), compound G4 (green) and compound G5 (blue).

Figure 7: DSSP program constitute secondary structure plot representing structural content (A) CAII, (B) complex CAII-compound G2, (C) complex CAII-compound G4, (D) complex CAII-compound G5 at 300 K of 50 ns MD simulation.

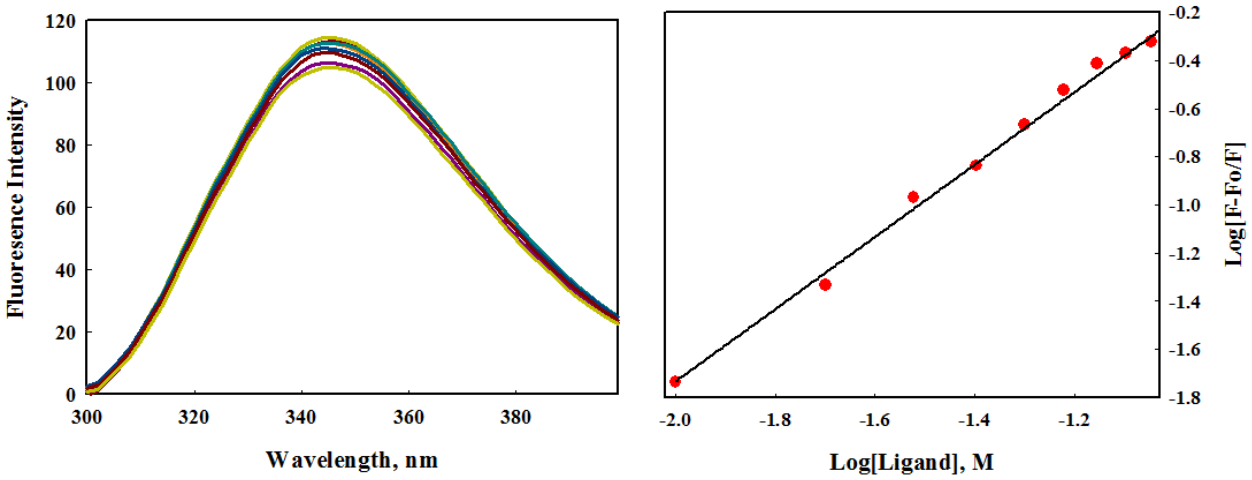

Fig. 1

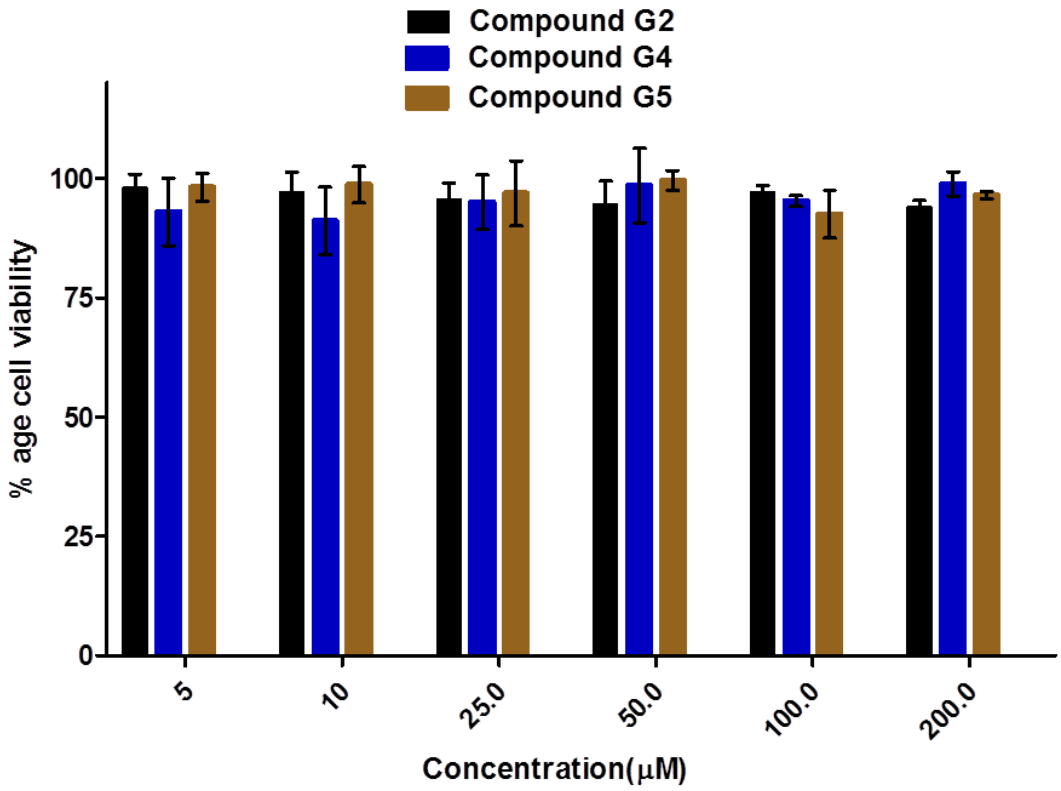

Fig. 2

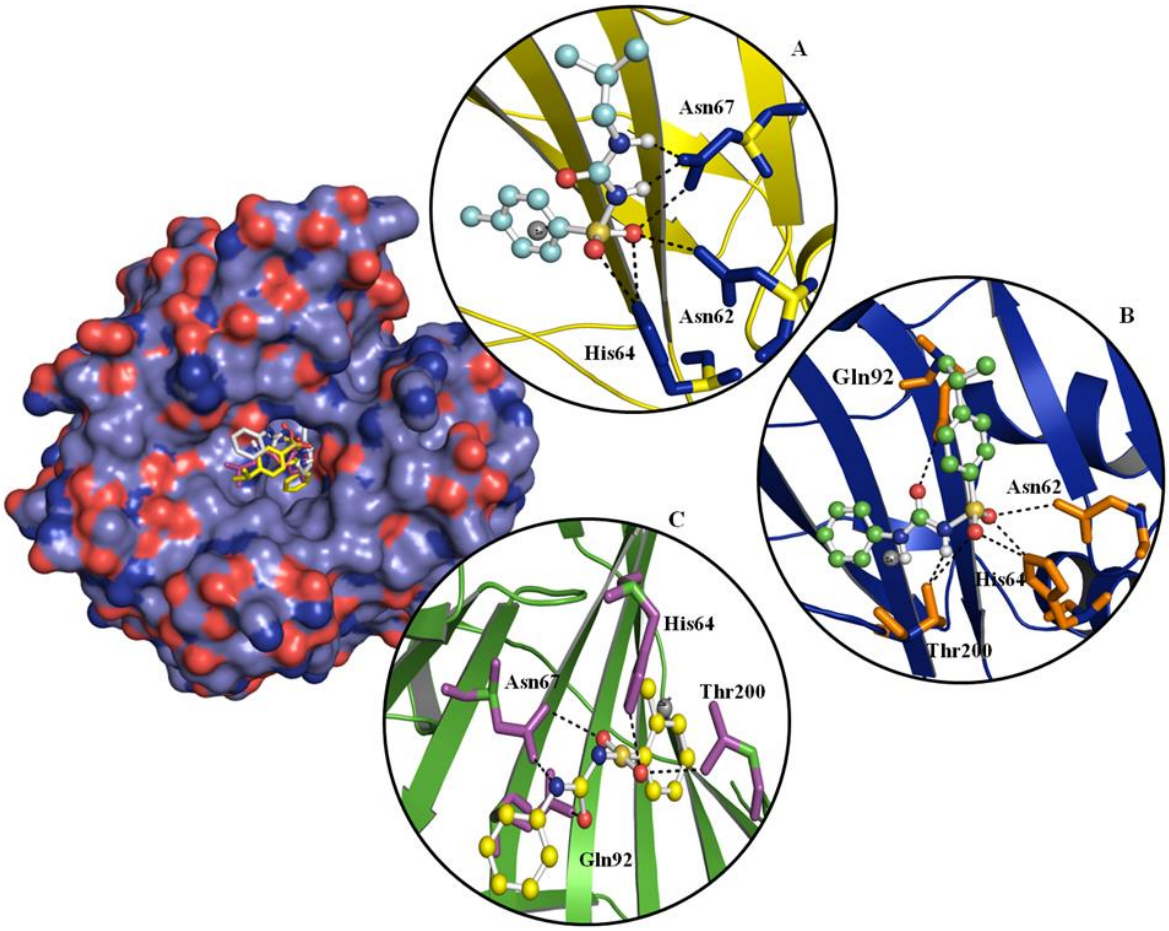

Fig. 3

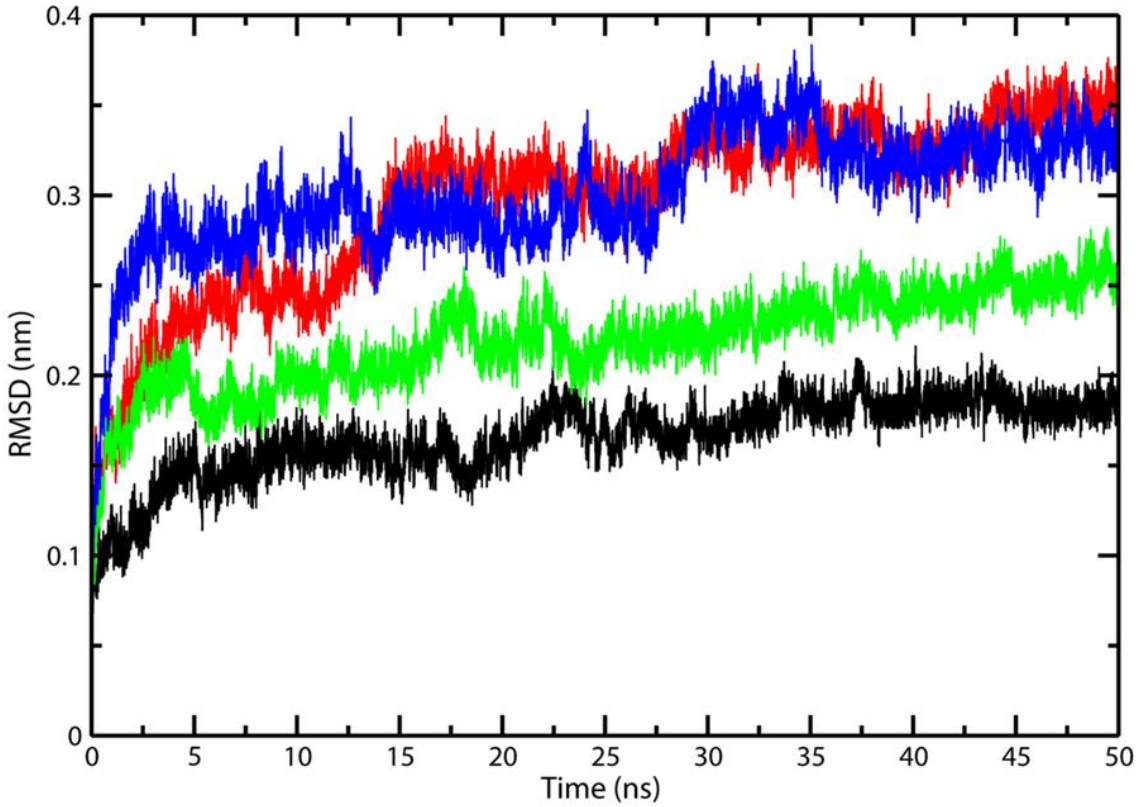

Fig. 4

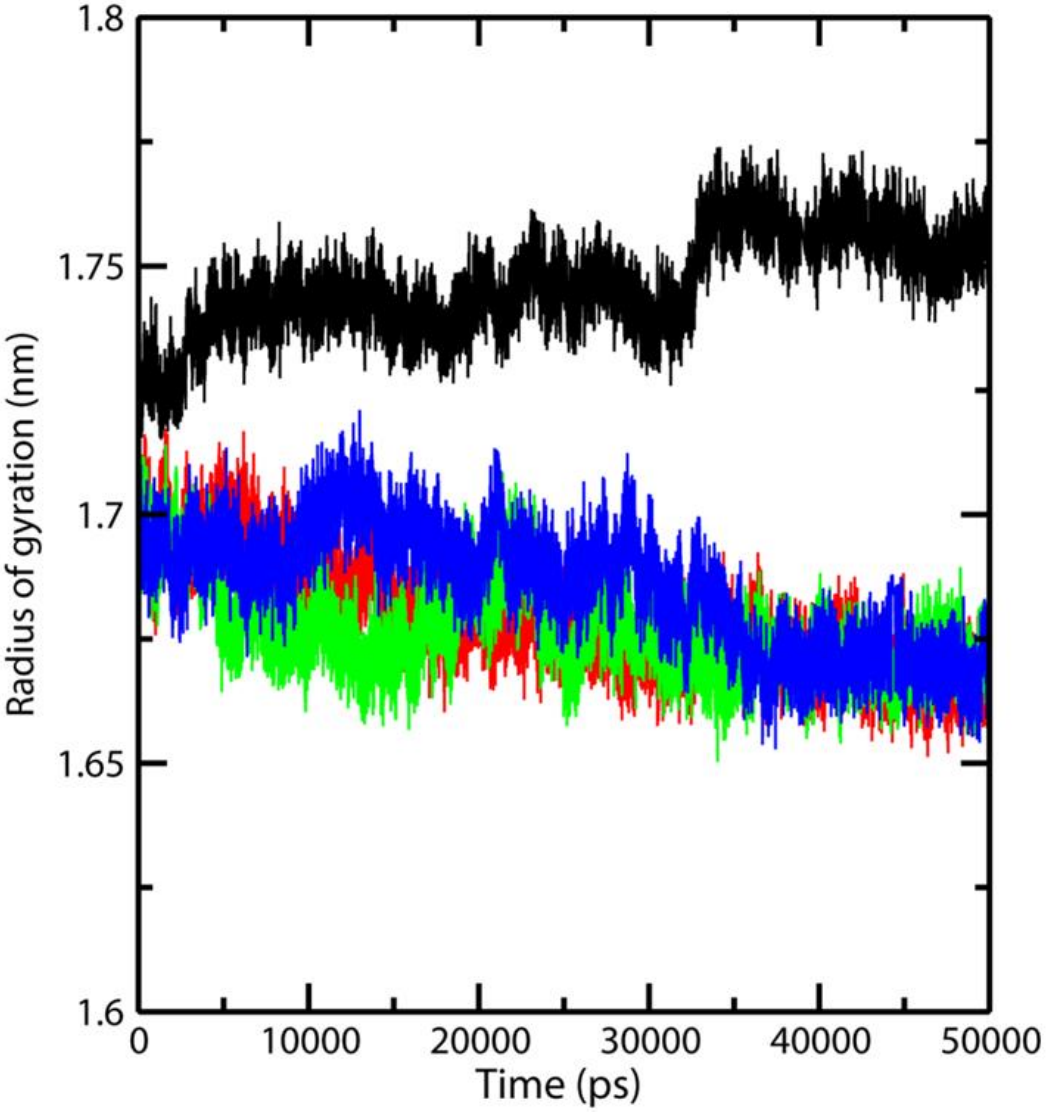

Fig. 5

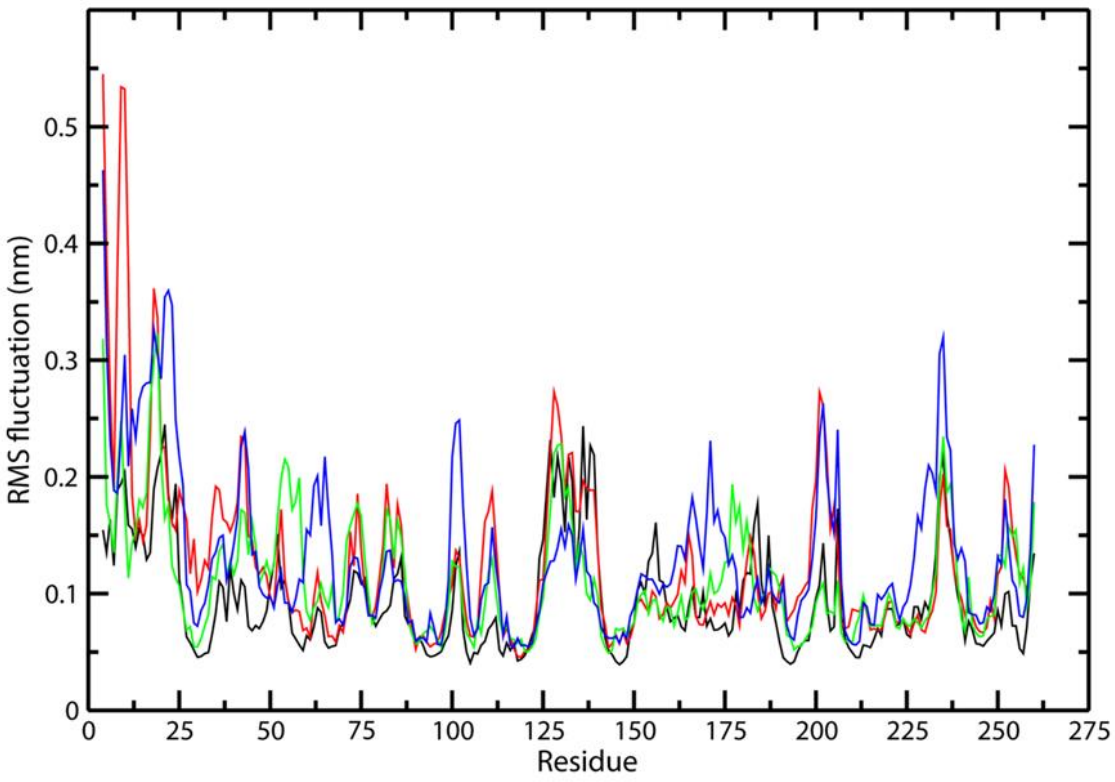

Fig. 6

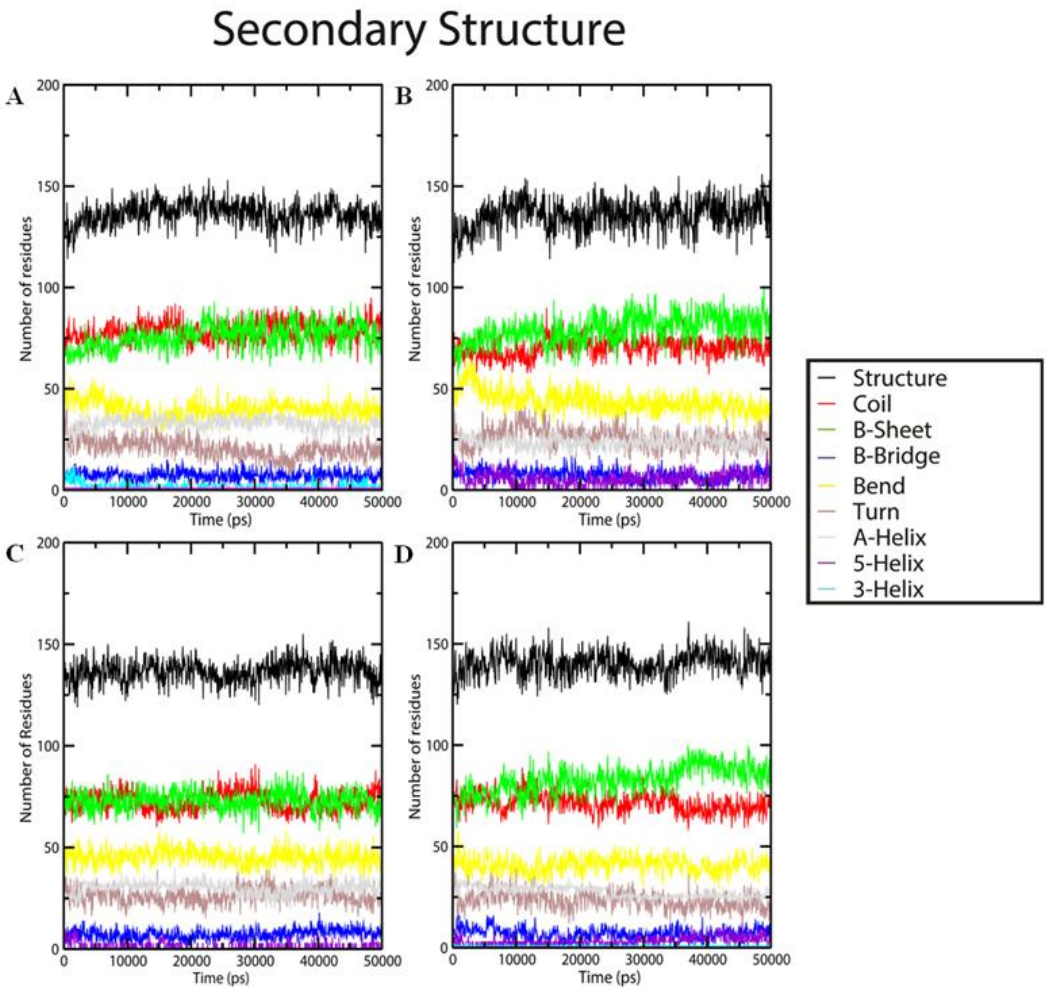

Fig. 7